A Novel Fabrication Approach for Improving the Efficiency of $FAPbI_3$ Based Perovskite Solar Cells

[1]N.Pirzada, [1]G. B. Narejo, [1]S. U. A. Shah and [2]T. A. K. Qasuria
[1]*Department of Electronic Engineering, NED University of Engineering & Technology, Karachi, 75270, Pakistan.*
[2]*Ghulam Ishaq Khan Institute of Engineering Sciences & Technology, Topi, Swabi, KPK, 23640, Pakistan.*
nomanpirzada@hotmail.com*****

(Received on 22nd December 2021, accepted in revised form 23rd February 2022)

Summary: The newly emerging perovskite solar cells (PSCs) embody excellent properties that are making them an attractive in photovoltaic (PV) technology. However, some shortcomings are impeding their commercial success. These include stability, efficiency, shelf life and operational life time. In this study, we attempted to overcome these shortcomings by exploring the fabrication by a modified spin coating approach where the dispensing of anti-solvent was optimized. Using Methyl Ammonium Formamidinium Lead Iodide as light harvester, several PSC devices were fabricated. For comparison, similar devices were also synthesized using a commonly used standard procedure. The devices were characterized for their I-V and P-V response using full sun solar simulator. Our results revealed that the fabrication approach based on optimized dispensing of anti-solvent resulted in considerable improvements in the efficiency with low production cost. In future, the approach can be adopted to overcome some of the problems associated with the current PSCs fabrication approaches.

Keywords: Perovskite solar cell, Photovoltaic, Electron transporting materials, Hole transporting materials, Power conversion efficiencies, Renewable energy, $FAPbI_3$, $MAPbI_3$, Spiro-OMeTAD.

Introduction

Considering the rapidly depleting conventional energy resources and the growing environmental concerns, our future depends on utilizing renewable energy sources [1]. Over the years, several technological advancements have emerged for the exploitation and utilization of ecofriendly renewable energy resources, such as solar, wind, geothermal, hydroelectric, biomass and biofuels [1]. Among them, solar energy is the most abundant, cleanest, low cost and inexhaustible source capable of meeting the energy demands of entire world [3]. Over the last few decades, solar cells or photovoltaics (PVs) have emerged as devices that can harvest solar energy and transform it into electrical energy [4].

Among the photovoltaic technologies available, the Perovskite Solar Cells (PSCs) based on organometallic halides represent the most promising photovoltaic technology owing to their better charge transport behavior, charge carrier, lifetime, higher absorption coefficient, excellent defect tolerance and low trap density [5, 6]. PSCs are now becoming attractive in terms of high efficiency and cost effective fabrication [7, 8].These materials showed appropriate optical and electrical properties for PV devices, such as tunable band gap, high optical absorption, long carrier diffusion length, and high defect tolerance [6, 9].

Over the last few years, PSCs have gained an unprecedented improvements in their efficiency from 4% to over 25% which is an impressive performance improvement compared to the other PV devices reported to date [10, 11]. However, it has been observed that efficiency and device stability are self-competing parameters [8, 12]. As a result, the World Economic Forum included PSCs in their list of top ten emerging technologies back in 2016. Since then, extensive efforts for their commercialization are started with the aim to make a major breakthrough in generating low cost, sustainable solar energy harvesters [13].

A basic perovskite solar cell (PSC) utilizes an organic-inorganic hybrid material based on lead or tin halide as light harvester. The charges (electrons and holes) travel separately towards corresponding electrodes via charge selective layers [14, 15]. The PSCs have a general chemical formula of AMX_3, in which the metallic cations (M) and anions (X) form MX_6 octahedra with the cations occupying coordinated holes of 12-folds within the cavity [15, 16].

Mostly, the perovskite materials used in PSCs are hybrid halides with a general formula ABX_3, where A represents a monovalent cation (such as Methyl Ammonium, Formamidinium, Cesium, Rubidium, or combinations of these), B represents a

***To whom all correspondence should be addressed.**

divalent cation (such as Tin, Lead and Germanium) and X represents a halide anion (I, Cl, Br, or their combinations) [16, 17].

Currently perovskite films are produced via solution based fabrication approaches using commonly available equipment [18]. The chemicals used in these fabrications are abundantly available and low cost, however, for most efficient devices, relatively expansive hole-transport materials, are needed [18, 19]. The PSC structure includes layers of transparent conductive oxide(TCO),coated substrate (glass), an electron transport layer (ETL/ETM) (n-type semiconductor), an absorber perovskite layer, a hole-transport layer (HTL/HTM) (p-type semiconductor) and metal, TCO, or carbon based back-contact [18, 20]. In planar devices however, the absorber perovskite layer is often sandwiched between electron transport layer (such as compact TiO_2, SnO_2, or C_{60} and derivatives) and hole transport layer (such as Spiro-OMeTAD, poly (triarylamine), and poly(3,4-ethylenedioxythiophene)-poly(styrene sulfonate)) [20, 21]. Being still in their developing phase, the devices based on PSC are still less durable compared to silicon solar cells [22, 23]. The advantage, however, is their low cost and large scale manufacturing [7, 24]. Besides, the technology offers several advantages over traditional semiconductors, such as easy fabrication, excellent light absorption, tunable bandgaps and enhanced charge carrier mobilization [5, 7, 24].

The below layout demonstrates PSC working when an incident beam of photons hitting it.

Despite outperforming many commercially established photovoltaic technologies in terms of efficiency and cost effectiveness, there are still few shortcomings that need to be resolved before putting them into commercial applications [22, 25, 26]. For instance, the film absorption edge, even in highly efficient PSCs, is only around 800nm [27, 28]. Extensive efforts have already been initiated for the improvement. Some new designs are presented based on incorporating lead and tin containing $FA_{0.75}Cs_{0.25}Sn_{0.5}Pb_{0.5}I_3$and $MA_{0.5}FA_{0.5}Pb_{0.75}Sn0_{.25}I_3$ [29, 30] or by incorporating near infrared (NIR) absorbing solar cells in the tandem cell configuration [31]. Improved efficiencies have been obtained for easy oxidizable Tin based compositions which simulated increased research interest in this technology [13]. PSCs with better coefficient of light absorption are highly desirable due to their thickness and lightweight which make them suitable for flexible and portable devices, however, their short lifetimes (LT) hindered the commercialization efforts [32].

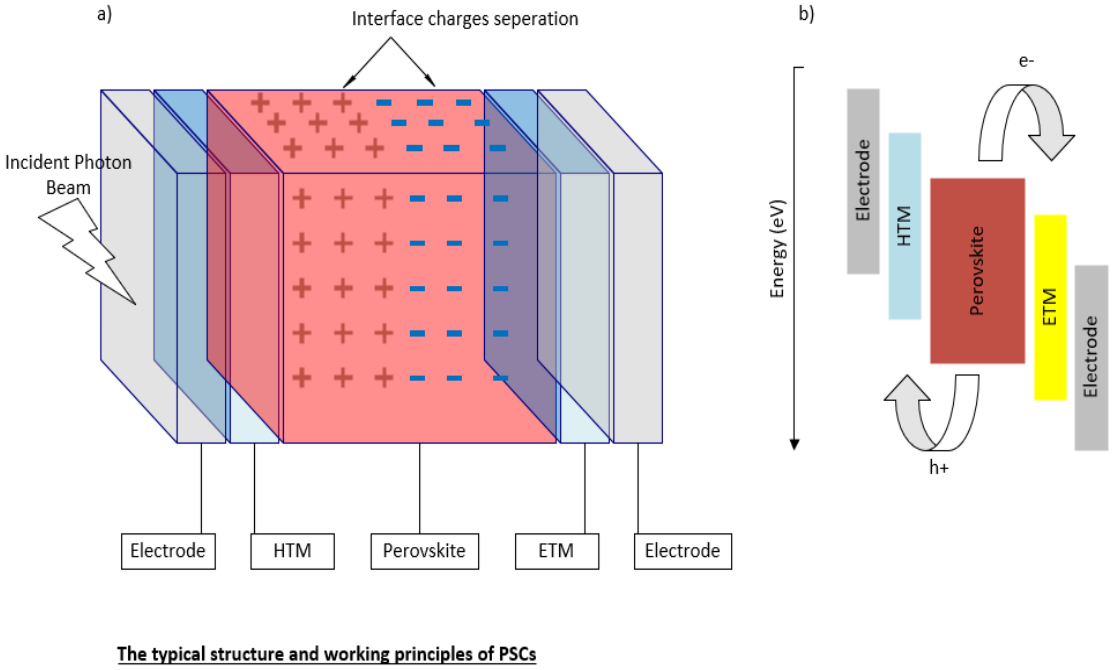

Layout 1: Typical structure of Perovskite Solar Cell and its working principal with incident photon beam.

The most challenging issue that hampered PSC commercialization is the low stability against various factors such as oxygen, moisture, light, electric field, temperature and also the film defects [32, 33]. Being a relatively new technology, the stability issues were remained unresolved. However, recently higher lifetimes of around 10,000 hours are reported under 1 kW/m^2 (1 sun) irradiation for printable mesoscopic PSCs [32]. The degradation of processes of halide perovskites are based on several correlated factors that originate from diverse sources such as heat, moisture, light, oxygen, and electrical bias [34, 35]. Low thermal stability is also a major problem associated with PSCs. In general, from the incident energy in solar radiation, only a small percentage, based on the conversion efficiency, is converted into electricity [7]. The remaining part of the absorbed energy is accumulated as heat and causes a considerable temperature, even 40^{o}C above ambient. This temperature rise is a critical problem which besides significantly influencing the performance, also accelerates degradation processes leading to drastically reduced lifetimes. Being organic-inorganic hybrids, the PSCs are even more susceptible to temperature rise effect and environmental conditions which drastically limit their life span. As the coefficient of thermal expansion for PSCs is considerably higher (over ten times that of glass and TCOs), the temperature rise provokes delamination [34, 36]. Another major problem is the temperature induced phase transition [37]. All these factors drastically affect the efficiency, shelf life and operational lifetime of PSCs.

As mentioned earlier, for the success of PSC technology, it is important to overcome these shortcomings, enhance the LT and minimize environmental impacts [7, 26, 32, 33]. The energy pay-back time (EPBT) is currently around 16.5 years with a life time of just 1 year. The EPBT can be substantially reduced just by increasing the life time which directly will minimize the impact of PSCs on the environment [38, 39]. Therefore, enhancing the lifetimes and stability of PSCs devices is highly desirable for successful commercialization. A solar cell must thermally and chemically be stable to sustain temperature changes and resist reactions with atmospheric molecules.

To date, several remedies are proposed to overcome the above mentioned shortcomings. Xiong et al. demonstrated that fixing of the perovskite grains by using phosphonic acid ammonium derivatives as crosslinkers impart considerable reduction in moisture sensitivity [40].The ingress of moisture is also observed to be reduced by the use of hydrophobic poly(methyl methacrylate)-carbon nanotube, nanocomposite and Teflon as these materials acted as barriers [2]. In another study carried out by Chen et al after around 670 hours, theOxo-G1 based solar cells showed 74% of the initial power conversion efficiency (PCE),whereas the PEDOT:PSS based cells retained only around 54% of the initial PCE [41]. Despite several approaches and fabrication methodologies that are reported in literature to improve the efficiency and stability of PSCs, there is still need for improvement. Methodologies adopted to make PSCs with over 20% efficiency in regular (n-i-p) and inverted (p-i-n) architectures have opened new doors for enhancing the performance and stability of PSCs [42–45].

In this paper we attempted a modified spin coating approach as shown in the flowchart under fabrication methodology, wherein the dispensing of anti-solvent was optimized. Using perovskite materials, $APbX_3$ (A = methylammonium (MA), formamidinium (FA), X = Br, I) several PSCs were fabricated. In past, although the use of these materials gave remarkable property improvement such as large carrier diffusion length and panchromatic absorption, tunable band gap and lower non radiative recombination rates, however the efficiencies of the resulting devices were considerably lower and the exposed electrode area was very small. As revealed by the results, the optimized anti-solvent dispensing approach resulted in considerable improvements in the efficiency with low production cost. We were able to achieve efficiency values as high as 14.725% under an exposed area of 1cm^2. We believe that the adopted approach can potentially overcome some of the problems associated with the current PSCs fabrication approaches.

Model & Methods

Power conversion efficiency of PSCs is calculated in two ways as shown in equation 1 and 2. Depending upon Open Circuit voltage, short circuit current, Fill factor, Incident light, maximum power and active area of cell under light source.

$$\textbf{Efficiency}(\eta) = \frac{\boldsymbol{Max\ or\ Peak\ Power}}{\boldsymbol{Incident\ Irradiance\ \times\ Device\ Area}} \times \mathbf{100}$$

Or

$$\eta = \frac{P_{max}}{E_{tot} * A} \boldsymbol{X100} \quad (1)$$

$$\eta = \frac{P_m}{P_{in}} = \frac{I_{sc} V_{oc}\, FF}{P_{in} A_{aperture}} = \frac{J_{sc} V_{oc}\, FF}{P_{in}} \quad (2)$$

where P_{in} is the incident light irradiance on the test cell, P_m is the maximum power output, $A_{aperture}$ is the aperture area exposed to the incident light, J_{sc} is Short circuit current density and I_{sc} is Short circuit current, V_{oc} is Open Circuit voltage, FF is Fill factor.

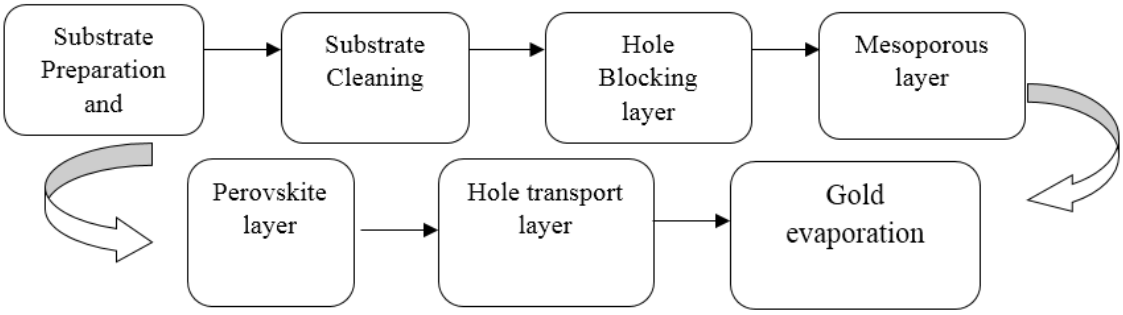

Fig. 1: Fabrication methodology of PSC with optimized technique of precursor dispensing opted in our research.

The performance efficiencies of solar cells are based on their *Fill Factor* which is the ratio of the maximum obtainable power, P_{max} to the product of short circuit current, I_{sc} and open circuit voltage, V_{oc} as in equation 3.

$$Fill\ Factor\ (FF) = \frac{P_{max}}{(I_{sc} \times V_{oc})} \quad (3)$$

The standard deviation is a measure of the amount of variation/dispersion in set of values and is given by equation.

$$SD = \sigma = \sum_1^n \frac{(x-\bar{x})^2}{n-1} \quad (4)$$

Experimental

Conventional methodology

The conventional methodology adopted for production of most PSCs involves FTO glass piece of 20x20mm which after cleaning and treating is covered with one fifth of its surface with a tape and placing it on a Spin coater at 1000 to 1500 rpm and after dropping 4 to 5 drops of Titanium Dioxide precursor solution rotate it from 3500 to 4000rpm and allow it to spin for 10 seconds to 1 minute. After removing tape, subject it to sintering at 450°C for 10 min and then allowing it to cool down for another 10 min. Then again covering a small portion of FTO glass facing Titanium surface and putting it on Hot plate at 110°C for 10 min and subjecting it to a Glove box for spin coating at 3000rpm with few drops of $MAPbI_3$ or $FAPbI_3$ precursor solution for 45 seconds. This completes the deposition of Perovskite layer on it.

Optimized methodology

Materials employed

FTO glass substrates (2.2mm TEC15) were purchased from (Pilkigton, Reagents Tri [bis (trifluoromethane) sulfonamide (FK209, Sigma Aldrich), 4-tert-Butylpyridine (TBP, Sigma Aldrich), Titanium diisopropoxide bis (acetylacetonate) (Sigma Aldrich), 30NRD (Dyesol) (Sigma Aldrich), TiO_2 (Sigma Aldrich), Spiro-OMeTAD (Merck) were all analytical grade and used as received. Precursor solution with FAI (1 M), PbI_2 (1.1 M) and $PbBr_2$ (0.22 M) TCI Dyenamo products and used as received. Solvents ethanol (Sigma Aldrich), Dimethylformamide (DMF), Dimethyl sulfoxide (DMSO), $MABr_2$ were all received from Sigma Aldrich and used without further purification. For all experiments, Deionized water (DI, 2%, Hellmanex) was used.

Test Cell Fabrication

1) Substrate Preparation and Patterning: Fluorine doped Tin Oxide (FTO) Glass (2.2mm TEC15 by Pilkigton) was finely cut in tiles with a diamond cutter in a size of 20x20mm. The FTO glass was patterned by chemical etching to get coated for a desired pattern. Kapton tape as Etch resistant was applied delicately on conductive surface. It was done by leaving 6~7mm surface exposed from one edge and completely laminating the rest to cover it. Zinc powder was uniformly dispersed on the exposed FTO with the help of a spatula. Leaving the exposed FTO, by using a cotton bud, the rest of the Zinc Powder was removed. A solution of 3M HCl was precisely dropped on that part of zinc powder till the point when we didn't notice any generation of bubbles and then it was left for 10 minutes). For the cleaning of glass tiles, those were washed using a soft brush immersed in soapy tap water and later rinsed with deionized water.
2) Substrate Cleaning: For the ultrasonic cleaning of those patterned tiles, they were placed vertically in a sonicator with Hellmanex/DI water (2%) and left it for 20 min, then immersed for another 20 min in Isopropyl Alcohol (IPA). Dried them with clean dried air/nitrogen and later placed for 20 min under an Ozone lamp.

3) Hole Blocking layer: We used spray pyrolysis at 450°C by using a precursor solution of titanium diisopropoxide bis (acetylacetonate) (0.025 M in anhydrous ethyl Alcohol) to achieve a compact hole blocking layer which was deposited on a pre-heated hot plate using a steady hand placed at about a distance of 20 cm from the FTO substrate (make 3, passes only). After spraying, the substrates were placed on hot plate for 45 min to heat at 450°C and then cooled down gently to room temperature.
4) Mesoporous layer: A TiO_2 suspension (30-NRD by Dyesol) was prepared in Ethyl Alcohol (1:5), and the mixture was stirred vigorously for 120 min before depositing by spin-coating (at 5000 rpm for 0.5 min). Dried substrate was then put on hotplate with lid closed to get uniform temperature distribution and sintered at 500°C for 30 min (Ramp rate of 100°C/min), after this substrate were allowed to cool down until 150°C and moved then in a glovebox with inert atmosphere. TiO_2 mesoporous layer thickness with this is achieved to 180 +/-20nm. Once again Kapton tape was applied to protect the contact area prior to spin-coating of perovskite for hole transporting material (HTM). It is applied on both side of mp-TiO_2 to avoid cleaning of HTM on perovskite on FTO before coating of gold contact layer by evaporation.
5) Perovskite layer: In the glove box, mixed perovskite layer was deposited using a precursor solution comprising FAI (01 M), PbI_2 (1.1 M), MABr (0.2 M) and $PbBr_2$ (0.22 M) in 4:1 (v:v) mixture of anhydrous DMF and DMSO. The perovskite solution was spin-coated (Laurell Technologies Corporation Model: WS-MZ) in two steps. First at 1,000 rpm and then at 6,000 rpm. for 10 and 30 seconds, respectively. In the second step, 150 µl of anti-solvent chlorobenzene was introduced on the spinning substrate just before 15 seconds to the ending of the spinning cycle. The substrates were then cured at 100 °C for 1 hour under inert atmosphere in a glove box.
6) Hole transport layer: After thorough cleaning of Spin coating and flushing with Nitrogen, Hole transport layer was deposited by spin coating. Following is the formulation used for hole transport layer solution.
7) Formulation130 mg bis(trifluoro methane) sulphonamide lithium salt (Li-TFSI) was dissolved in 0.250 mL acetonitrile; 1.811M in a glass vial and labelled it as (solution A). Then in a second vial 50 mg tris(2-(1H-pyrazol-1-yl)-4-tertbutylpyridine) cobalt(III) tri[bis(trifluoro methane) sulphonamide] (FK209, Aldrich), was dissolved in 100 µL acetonitrile; 0.108M) and labelled it as (solution B). Then using a separate vial with 147.05 mg Spiro-OMeTAD was dissolved in 1.36 mL chlorobenzene and labelled it as (solution C). To solution C above we used 36.5 µL of solution A and 29.4 µL of solution B, followed by 57µL 4-tert-Butylpyridine to prepare hole transport stock solution. The stock solution was prepared a day prior to use. 50 µL of hole transport solution was spin-coated at 4000 rpm for 30 sec on the perovskite layer and then was dried for 30 min in the glovebox.

From both sides Kapton tape was removed prior to gold evaporation.

8) Gold evaporation was carried out in the metal evaporator: Gold film was deposited upto 70-80nm, by moving subjecting devices to the high vacuum metal evaporator for thermal evaporation.

Characterization:

The PSCs were measured using a 450 Watt Xenon light (Oriel) in a solar simulator by Newport. The spectral mismatch of AM1.5G and simulated illumination was reduced by the use of a Tempax filter Schott K113 from Präzisions Glas& Optik GmbH. A Si photodiode having an IR-cutoff filter (KG3, Schott) was used for calibration of the light intensity, and the data obtained from it was recorded during each measurement. An external voltage bias was applied with the help of Solar simulator to record Current-voltage characteristics of the cells by simultaneously measuring the current response from a digital source meter (Keithley 2400). The voltage scan rate was set to 10 mV/s without any device preconditioning, such as extended forward voltage biasing or light soaking in dark. The intensity of incident light was tuned to 1000 W/m^2following the standard AM 1.5 to comply with.

Result and Discussion

All the PSC devices were fabricated using perovskite materials, $APbX_3$ (A = methylammonium (MA), formamidinium(FA), X = Br, I)on Fluorine doped Tin Oxide (FTO) substrates. As mentioned earlier, a modified spin-coating approach was adopted wherein we utilized optimized dispensing of antisolvent. Initially, few nanometer thick hole blocking layer of mesoporous TiO_2 was spin-coated as an electron selective contact. The spin coated layer was then subjected to sintering to get the desired morphology and the thickness of around 180 ± 20 nm was finally achieved. The hole transport layer was also spin coated, as mentioned in the experimental section. All the devices were gold coated with a 70-80 nm thick layer acted as the counter electrode. The approach resulted in considerable improvements and efficiency as high as 14.725% under an exposed area of $1cm^2$was achieved which is a

significant improvement compared to the PSC devices reported in the literature in comparison to other obtained efficiencies with different active areas [10, 44–46]. It has been observed that if active area increases, the efficiency drops down drastically as in Table-1.

Table-1 is based on the outputs obtained from various techniques of optimized dispensing methods and exposed with various active cell areas. Most of the experimentations uses 0.09cm^2 of active cell area but as soon as we increase it, the efficiency drops down because of the nonuniformity of layers over wide area. This is one of the reasons that commercial production of photovoltaic cells is far below their reported lab-scale efficiency. The maximum efficiency achieved with an active area of 1cm^2 is 12%.

The photovoltaic behavior of the PSC devices was studied by measuring their Current-Voltage characteristics. During the measurements, the bias voltage was swept in small steps and the resulting photocurrent was monitored simultaneously. A number of key parameters related to the device performance can be extracted from these measurements. These include short-circuit current, current density, open-circuit voltage, fill factor and power conversion efficiency. The relationship among these parameters is given by the equation 1 and 2 for efficiency calculation [28].

The performance of a solar cell is often evaluated by measuring the Current-Voltage (I-V) curves. The I-V curves obtained for the PCS device fabricated using the optimized anti-solvent dispensing is shown in Fig. 2. Clearly, a hysteresis is observed between forward and reverse scans. For comparison, I-V curves (both forward and reverse scans) of the PSC device obtained using standard procedures are also shown in Fig 2. It should be noted that the forward and reverse curves of the PCS device fabricated using the optimized dispensing of anti-solvent exhibit better overlapping with significantly low hysteresis, compared to the PSC device obtained using a standard procedure. The observed hysteresis in the shape of the I-V curves is likely originated from the capacitance of the solar cell [51, 52]. During short-circuit to forward bias scanning, the cell can charge resulting in an extra-capacitive charge along with the photogenerated charge, extracted in the reverse scan. This effect is more pronounced when sweeping is done very rapidly [51]. In this case, the photogenerated charge can partially charge the cell which in turn reduces the amount of charge flowing into the external circuit. The changes in the current measured in the forward and reverse mode resulted in hysteresis in the obtained IV curves.

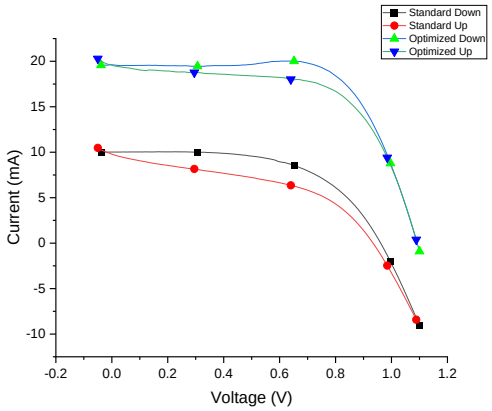

Fig. 2: Current-Voltage (IV) plots of the PSC devices fabricated using conventional standard (red circles: forward scan; black squares: reverse scan) and anti-solvent optimized (blue inverted triangles: forward scan; green triangles: reverse scan) procedure.

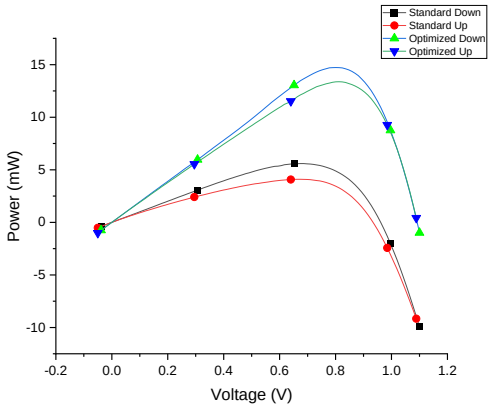

Fig. 3: Power-Voltage (P-V) plots of the PSC devices fabricated using conventional standard (red circles: forward scan; black squares: reverse scan) and anti-solvent optimized (blue inverted triangles: forward scan; green triangles: reverse scan) procedure.

Fig. 3 shows both forward and reverse scans of the Power-Voltage (P-V) curves obtained for the PCS device fabricated using the optimized dispensing of anti-solvent. For comparison, P-V curves obtained for the device fabricated using a standard procedure are also included. The P-V power conversion efficiency is the most common performance indicator for PV cells. Under standard operating conditions the power conversion efficiency is defined as the ratio of maximum output (electric) to the total irradiance.[53].

Table-1: Reported efficiencies for FAPbI3.

Efficiency	21%	14.2%	17.3%	12%	8.3%	14.725%
Active Area	0.090cm^2	0.092cm^2	0.16cm^2	1cm^2	0.090cm^2	1cm^2
References	[47]	[48]	[49]	[50]	[50]	As reported in our research

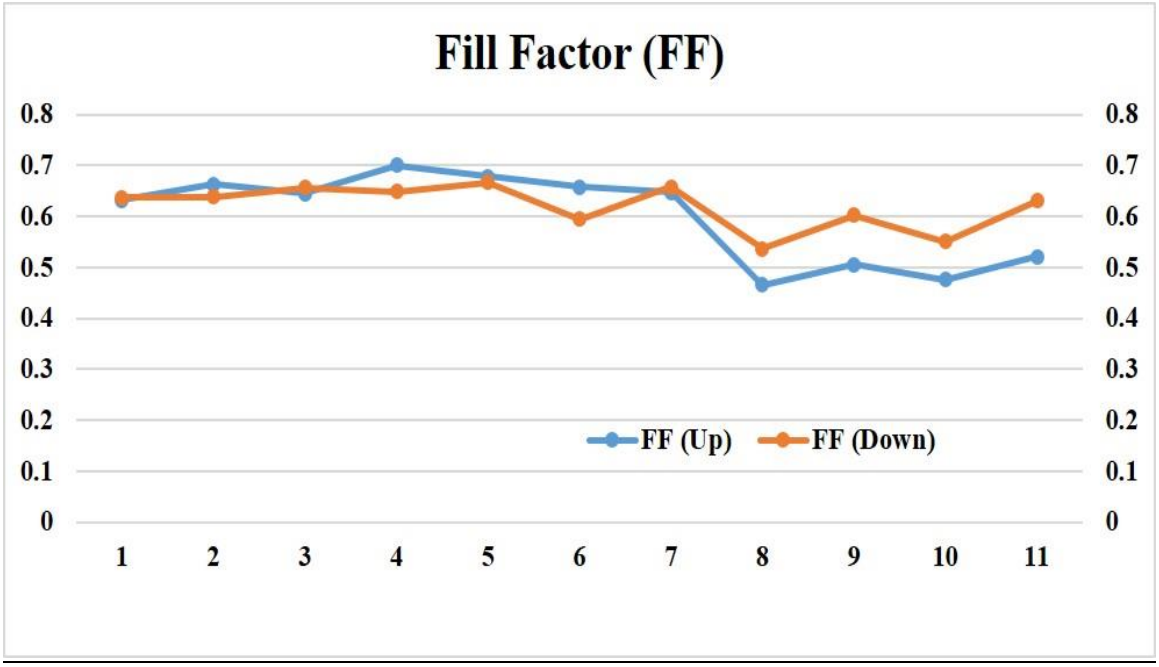

Fig. 4: Fill factor calculated for several PSC devices fabricated using anti-solvent optimized procedure (both forward reverse scans are shown).

As can be seen in Fig 3, for the cell fabricated using standard procedure, the maximum power efficiency achieved under solar simulator for both forward and reverse scans, was turned out to be only around 5%. These values are in fair agreement with the values reported in literature and clearly showing that the conventional fabrication approaches are less efficient. The low efficiency is likely due to several imperfections and limitations in the quality of perovskite layer such as grain size, packing and intimate contact with the subsequent layers. These factors affect charge extraction hence limiting PSC performance adversely[54]. The P-V curves of the PSC devices fabricated by optimized anti-solvent dispensing approach is also shown in Fig 3. Remarkably, efficiency value above 14.725% for an active area of 1 cm^2 is achieved which is a considerable improvement compared to the conventional procedures. The performance efficiencies of solar cells are often compared by calculating the *Fill Factor* which is the ratio of the maximum obtainable power to the product of short circuit current and circuit voltage. FF is a ratio and calculated using equation 3.

To evaluate the performance efficiency, the Fill Factors of several PCS devices fabricated using optimized anti-solvent dispensing approach are calculated and the results are depicted in Fig 4 (results for both forward and reverse scans are included). For most of the devices, the values of the Fill Factor lie within the range of 0.6 to 0.7 demonstrating excellent efficiency and reproducibility. The maximum power values for forward and reverse scans along with the standard deviations for all PSCs are plotted in Fig 5. These results were obtained for number of devices and clearly indicating enhanced performance for each PSC device. It can therefore be concluded that using better opulent cleaning processes, vigilant application procedures and careful spin-coating technique by optimizing the anti-solvent dispensing high efficiency PSC devices can be fabricated devices. There is a possibility to elevate the efficiency even further by a comprehensive process optimization

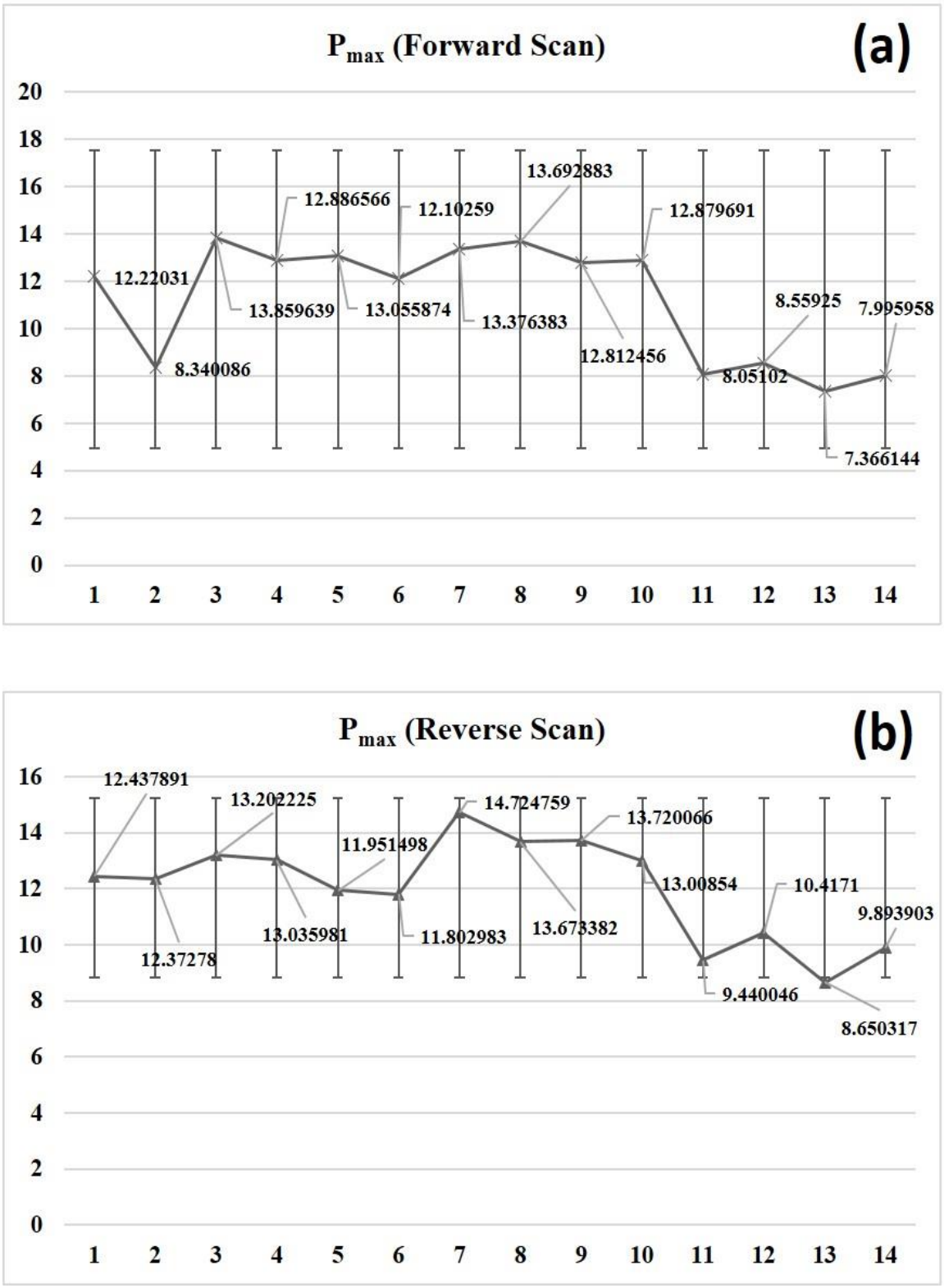

Fig. 5: Maximum power plots with standard Deviation & Error bars for several PSC devices fabricated using anti-solvent optimized procedure (both forward reverse scans are shown), calculated using equation 4.

Table-2: Analysis parameters of PSCs after optimization.

Scan Direction	FF	Efficiency	Voc	Isc	Pmax	Vmp	Imp	Area	Sun Level
Down	0.6870	14.72476	1.0919	19.628	14.725	0.801	18.383	1	1
Up	0.6242	13.376382	1.0921	19.622	13.376	0.8125	16.463	1	1

Conclusion

In summary, we demonstrated the effectiveness of a novel fabrication approach for the fabrication of very efficient perovskite solar cells. The approach is based on a modified spin coating technique where the dosing of the anti-solvent is optimized in dispensing technique and spinning speed. Our results revealed that the approach was successful in achieving considerable efficiency improvement. Compared to the conventional procedure, the PCS devices fabricated using the optimized anti-solvent dispensing procedure exhibit considerably less hysteresis in the forward and reverse scans of the IV and PV curves. Besides the high P_{max} values and consistent fill factors indicate their superior performance.

In conclusion, the novel optimized anti-solvent dispensing approach resulted in considerable efficiency improvements with low production cost and high reproducibility. In future, the approach can be further improved and adopted commercially to overcome the present problems associated with the conventional fabrication routes.

References

1. M. B. Hayat, D. Ali, K. C. Monyake, L. Alagha and N. Ahmed. Solar energy—A look into power generation, challenges, and a solar-powered future, *Int. J. Energy Res.*, **43**, 1049 (2019).
2. S. N. Habisreutinger, T. Leijtens, G.E. Eperon, S. D. Stranks, R. J. Nicholas and H. J. Snaith. Carbon nanotube/polymer composites as a highly stable hole collection layer in perovskite solar cells, *Nano Lett.*, **14**, 5561 (2014).
3. M. A. G. De Brito, L. P. Sampaio, L. G. Junior and C. A. Canesin. *Research on photovoltaics: review, trends and perspectives*. XI Brazilian Power Electron. Conf., p. 531 (2011).
4. M. H. Shubbak. Advances in solar photovoltaics: Technology review and patent trends, *Renew. Sustain Energy Rev.*, **115**, 109383 (2019).
5. M. I. H. Ansari, A. Qurashi and M. K. Nazeeruddin. Frontiers, opportunities, and challenges in perovskite solar cells: A critical review, *J. Photochem. Photobiol. C Photochem. Rev.*, **35**, 1 (2018).
6. M. L. Petrus, J. Schlipf, C. Li, T. P. Gujar, N. Giesbrecht, P. Müller-Buschbaum, *et al*. Capturing the sun: A review of the challenges and perspectives of perovskite solar cells, *Adv. Energy Mater.*, **7**, 1700264 (2017).
7. M. A. Green, A. Ho-Baillie and H. J. Snaith. The emergence of perovskite solar cells, *Nat. Photonics*, **8**, 506 (2014).
8. S. Yang, W. Fu, Z. Zhang, H. Chen and C.- Z. Li. Recent advances in perovskite solar cells: efficiency, stability and lead-free perovskite, *J. Mater. Chem A.*, **5**, 11462 (2017).
9. M. Kumar and A. Kumar. Performance assessment and degradation analysis of solar photovoltaic technologies: A review, *Renew. Sustain Energy Rev*., **78**, 554 (2017).
10. E. Akman, A. E. Shalan, F. Sadegh and S. Akin. Moisture-Resistant FAPbI3 Perovskite Solar Cell with 22.25\% Power Conversion Efficiency through Pentafluorobenzyl Phosphonic Acid Passivation, *ChemSusChem.*, **14**, 1176 (2021).
11. X. Ding, H. Wang, C. Chen, H. Li, Y. Tian, Q. Li, *et al*. Passivation functionalized phenothiazine-based hole transport material for highly efficient perovskite solar cell with efficiency exceeding 22%, *Chem. Eng. J.*, **410**, 128328 (2021).
12. M. Ye, X. Hong, F. Zhang and X. Liu. Recent advancements in perovskite solar cells, flexibility, stability and large scale, *J. Mater. Chem. A*, **4**, 6755 (2016).
13. G. Agenda. Top 10 Emergin Technologies of 2016 (2016).
14. N-. G. Park. Perovskite solar cells, an emerging photovoltaic technology, *Mater. Today*, **18**, 65 (2015).
15. P. P. Boix, K. Nonomura, N. Mathews and S.G. Mhaisalkar. Current progress and future perspectives for organic/inorganic perovskite solar cells, *Mater. Today*, **17**, 16 (2014).
16. P. P. Boix, S. Agarwala, T. M. Koh, N. Mathews and S. G. Mhaisalkar. Perovskite solar cells: beyond methylammonium lead iodide, *J. Phys. Chem. Lett.*, **6**, 898 (2015).
17. L. Yang, X. Wang, X. Mai, T. Wang, C. Wang, X. Li, *et al.* Constructing efficient mixed-ion perovskite solar cells based on TiO2 nanorod array, *J. Colloid. Interface Sci.*, **534**, 459 (2019).
18. A. Dubey, N. Adhikari, S. Mabrouk, F. Wu, K. Chen, S. Yang, *et al*. A strategic review on processing routes towards highly efficient perovskite solar cells, *J. Mater. Chem. A*, **6**, 2406 (2018).
19. L. Calió, S. Kazim, M. Grätzel and S. Ahmad. Hole-transport materials for perovskite solar cells, *Angew Chemie Int. Ed.*, **55**, 14522 (2016).

20. H. S. Jung and N-. G. Park. Perovskite solar cells: from materials to devices, *Small*, **11**, 10 (2015).
21. H. Yoon, S. M. Kang, J-. K. Lee and M. Choi. Hysteresis-free low-temperature-processed planar perovskite solar cells with 19.1\% efficiency, *Energy \& Environ. Sci.*, **9**, 2262 (2016).
22. X. Zhao and N-. G. Park. Stability issues on perovskite solar cells, *Photonics*, **2**, 1139 (2015).
23. H-. S. Kim, J-. Y. Seo and N-. G. Park. Material and device stability in perovskite solar cells, *ChemSusChem*, **9**, 2528 (2016).
24. A. Mutalikdesai and S. K. Ramasesha. Emerging solar technologies: Perovskite solar cell, *Resonance*, **22**, 1061 (2017).
25. A. B. Djurišić, F. Z. Liu, H. W. Tam, M. K. Wong, A. Ng, C. Surya, *et al*. Perovskite solar cells-An overview of critical issues, *Prog. Quantum Electron*. **53**, 1 (2017).
26. P. Roy, N. K. Sinha, S. Tiwari and A. Khare. A review on perovskite solar cells: Evolution of architecture, fabrication techniques, commercialization issues and status, *Sol. Energy*, **198**, 665 (2020).
27. M. A. Green, Y. Hishikawa, E. D. Dunlop, D. H. Levi, J. Hohl-Ebinger and A. W. Y. Ho-Baillie. Solar cell efficiency tables (version 52), *Prog. Photovoltaics Res. Appl.*, **26**, 427 (2018).
28. Y. Wang, X. Liu, Z. Zhou, P. Ru, H. Chen, X, Yang, *et al*. Reliable measurement of perovskite solar cells, *Adv. Mater.*, **31**, 1803231 (2019).
29. Z. Yang, A. Rajagopal, C-. C. Chueh, S. B. Jo, B. Liu and T. Zhao, *et al*. Stable Low-Bandgap Pb--Sn Binary Perovskites for Tandem Solar Cells, *Adv. Mater.*, **28**, 8990 (2016).
30. G. E. Eperon, T. Leijtens, K. A. Bush, R. Prasanna, T. Green, J. T-. W. Wang, *et al*. Perovskite-perovskite tandem photovoltaics with optimized band gaps, *Science* (80-), **354**, 861 (2016).
31. J. Werner, L. Barraud, A. Walter, M. Bräuninger, F. Sahli, D. Sacchetto, *et al*. Efficient near-infrared-transparent perovskite solar cells enabling direct comparison of 4-terminal and monolithic perovskite/silicon tandem cells, *ACS Energy Lett.*, **1**, 474 (2016).
32. Y. Rong, Y. Hu, A. Mei, H. Tan, M. I. Saidaminov, S. Seok Il, *et al*. Challenges for commercializing perovskite solar cells, *Science* (80-), 361 (2018).
33. L. K. Ono, N-. G. Park, K. Zhu, W. Huang and Y. Qi. Perovskite Solar Cells Towards Commercialization, *ACS Energy Lett*., **2**, 1749 (2017).
34. C. C. Boyd, R. Cheacharoen, T. Leijtens and M. D. McGehee. Understanding degradation mechanisms and improving stability of perovskite photovoltaics, *Chem. Rev.*, **119**, 3418 (2018).
35. J. Bisquert and E. J. Juarez-Perez. The causes of degradation of perovskite solar cells (2019).
36. Y. Zhao, D. J. Weidner, J. B. Parise and D. E. Cox. Thermal expansion and structural distortion of perovskite—data for NaMgF3 perovskite, *Part I. Phys. Earth. Planet Inter.*, **76**, 1 (1993).
37. C. A. Triana, L. T. Corredor, D. A. L. Téllez and J. Roa-Rojas. High temperature-induced phase transitions in Sr2GdRuO6 complex perovskite, *Mater. Res. Bull.*, **46**, 2478 (2011).
38. V. Fthenakis and E. Leccisi. *Life-Cycle Analysis of Tandem PV Perovskite-Modules and Systems*. 2021 IEEE 48th Photovolt. Spec. Conf., 1478 (2021).
39. R. Wang, M. Mujahid, Y. Duan, Z. K. Wang, J. Xue and Y. Yang. A Review of Perovskites Solar Cell Stability, *Adv. Funct. Mater*. **29**, 1 (2019). https://doi.org/10.1002/adfm.201808843.
40. X. Li, M. I. Dar, C. Yi, J. Luo, M. Tschumi, S. M. Zakeeruddin, *et al*. Improved performance and stability of perovskite solar cells by crystal crosslinking with alkylphosphonic acid $ω$-ammonium chlorides, *Nat. Chem.*, **7**, 703 (2015).
41. H. Chen, Y. Hou, C. E. Halbig, S. Chen, H. Zhang, N. Li, *et al*. Extending the environmental lifetime of unpackaged perovskite solar cells through interfacial design, *J. Mater. Chem. A*, **4**, 11604 (2016).
42. F. Sadegh, S. Akin, M. Moghadam, R. Keshavarzi, V. Mirkhani, M. A. Ruiz-Preciado, et al. Copolymer-Templated Nickel Oxide for High-Efficiency Mesoscopic Perovskite Solar Cells in Inverted Architecture, *Adv. Funct. Mater.*, 2102237 (2021).
43. T. Ozturk, E. Akman, A. E. Shalan and S. Akin. Composition engineering of operationally stable CsPbI2Br perovskite solar cells with a record efficiency over 17\%, *Nano Energy*, **87**, 106157 (2021).
44. A. E. Shalan, E. Akman, F. Sadegh and S. Akin. Efficient and stable perovskite solar cells enabled by dicarboxylic acid-supported perovskite crystallization, *J. Phys. Chem. Lett.*, **12**, 997 (2021).
45. S. Akin, E. Akman and S. Sonmezoglu. FAPbI3-Based Perovskite Solar Cells Employing Hexyl-Based Ionic Liquid with an Efficiency Over 20\% and Excellent Long-Term Stability, *Adv. Funct. Mater.*, **30**, 2002964 (2020).
46. Y. Liu, S. Akin, A. Hinderhofer, F. T. Eickemeyer, H. Zhu, J-. Y. Seo, *et al*. Stabilization of highly efficient and stable phase-pure FAPbI3 perovskite solar cells by molecularly tailored 2D-overlayers, *Angew. Chemie. Int. Ed.*,

59, 15688 (2020).
47. S. S. Mali, J. V. Patil, H. Arandiyan and C. K. Hong. Reduced methylammonium triple-cation Rb 0.05 (FAPbI 3) 0.95 (MAPbBr 3) 0.05 perovskite solar cells based on a TiO 2/SnO 2 bilayer electron transport layer approaching a stabilized 21\% efficiency: the role of antisolvents, *J. Mater. Chem. A*, **7**, 17516 (2019).
48. J. Borchert, R. L. Milot, J. B. Patel, C. L. Davies, A. D. Wright, L. Martínez Maestro, *et al*. Large-area, highly uniform evaporated formamidinium lead triiodide thin films for solar cells, *ACS Energy Lett.*, **2**, 2799 (2017).
49. N. J. Jeon, J. H. Noh, W. S. Yang, Y. C. Kim, S. Ryu, J. Seo, *et al*. Compositional engineering of perovskite materials for high-performance solar cells, *Nature*, **517**, 476 (2015).
50. G. Hodes and D. Cahen. Perovskite cells roll forward, *Nat. Photonics*, **8**, 87 (2014).
51. H. J. Snaith, A. Abate, J. M. Ball, G. E. Eperon, T. Leijtens, N. K. Noel, *et al*. Anomalous hysteresis in perovskite solar cells, *J. Phys. Chem. Lett.*, **5**, 1511 (2014).
52. E. L. Unger, E. T. Hoke, C. D. Bailie, W. H. Nguyen, A. R. Bowring, T. Heumüller, *et al*. Hysteresis and transient behavior in current--voltage measurements of hybrid-perovskite absorber solar cells, *Energy \& Environ. Sci.*, **7**, 3690 (2014).
53. S. Collavini, S. F. Völker and J. L. Delgado. Understanding the outstanding power conversion efficiency of perovskite-based solar cells, *Angew. Chemie. Int. Ed.*, **54**, 9757 (2015).
54. Y. H. Lee, J. Luo, R. Humphry-Baker, P. Gao, M. Grätzel and M. K. Nazeeruddin. Unraveling the reasons for efficiency loss in perovskite solar cells, *Adv. Funct. Mater.*, **25**, 3925 (2015).